Surface integrity enhancement of turbine compressor blades using boron carbide abrasives in magnetic finishing: An experimental study

Tahseen Majed Salman[1]*, Saad. K. Shather[1], Baraa M. H. Albaghdadi[1]

[1] University of Technology, Al-Sina'a St., P.O. Box: 18310 Baghdad, Iraq
* Corresponding author's e-mail: pme.19.02@grad.uotechnology.edu.iq

ABSTRACT

This study looks at how well boron carbide (B4C), known for its outstanding hardness and heat resistance, works as an abrasive in the magnetic abrasive finishing (MAF) process to remove cracked layers from metal surfaces. The study focused on the surface integrity and rehabilitation of the compressor blade of a GE gas turbine that includes surface roughness, surface topology (microcracks), and the material removal rate after a period of service. Experimental work employed the Taguchi design with L9 trials in Minitab 17, involving three variables. The compressor blade is composed of AISI 403 stainless steel, and the MAF coil features 5200 turns of pure copper wire with a diameter of 0.6 mm and a cylindrical end pole. The results showed a significant improvement in surface topology, as analyzed by microscopic images taken before and after the MAF process. The best surface roughness improvement achieved was 38.99% when rotation speed was 800 r.p.m., gap distance was 1.8, and mixing ratio was 50%. The rate of microcrack removal was significantly improved, contributing to a more polished surface appearance. However, the process had a limited effect on larger cracks. According to Taguchi analysis, the abrasive mixing ratio parameter has the main or maximum effect on surface roughness, followed by rotation speed and the last gap distance. These results reflect the process's efficiency in removing microcracks, underscoring the importance of continuous surface evaluation to ensure early treatment before cracks expand and cause part failure.

Keywords: thermal fatigue, fatigue failure, MAF, B_4C powder, surface improvement, turbine blades.

INTRODUCTION

Finishing processes are essential techniques employed to improve the surface quality, functionality, and aesthetics of a workpiece following primary machining or forming operations. These processes emphasize achieving specific surface characteristics such as smoothness, precision, corrosion resistance, and durability, which are crucial for the functionality and longevity of components across various applications [1]. Removing fatigue crack layers is a critical application of magnetic abrasive finishing (MAF), as these layers are detrimental to the structural integrity of components subjected to cyclic stresses [2]. Magnetic abrasives, attracted to the surface, act like a flexible brush that polishes and smooths the material without causing damage [3–4]. This study examined the process of integrating B4C abrasive powder into the MAF to improve its performance. Boron carbide (B_4C) is a thermally stable and remarkably hard abrasive material utilized in advanced finishing processes, including magnetic abrasive finishing (MAF) [5–6].

The performance and longevity of turbine blades functioning in elevated temperature conditions are significantly affected by the surface properties of internal cooling channels. Progress in laser powder bed fusion (LPBF) has facilitated the production of complex internal geometries with tailored surface textures, presenting novel prospects for performance improvement. A recent extensive review by Jiang et al. (2025) [7] underscored the crucial significance of surface

topography in enhancing the thermal and mechanical properties of Inconel 718 turbine blades. The research highlighted that meticulously regulated surface roughness from LPBF can enhance turbulent flow, thus augmenting convective heat transfer while preserving acceptable pressure drop levels. Moreover, post-processing methods including laser re-melting, abrasive flow finishing, and micro-texturing demonstrably improve surface quality, thereby enhancing cooling efficiency and fatigue resistance. These insights underscore the necessity of incorporating surface topography factors into the design and production of next-generation turbine components.

In (2015), Zhou et al. [8] published a study that proposed integrating ultrasonic vibration with MAF to enhance efficiency and surface integrity in finishing titanium parts. The results showed ultrasonic MAF facilitates micro-removal of surface material and reduces or eliminates deterioration of surface lattice structure caused by milling forces. In the same year, Khangura et al. [9] studied the potential of MAF in removing the recast layers formed on cylindrical specimens (EN 31 steel) machined by electrical discharge machining (EDM). Experimental results show up to an 80% improvement in surface finish with no evidence of the micro-cracks, voids, or recast layers on the finished surfaces. In 2019, Zhang et al. [10] investigated MAF of selective-laser-melted 316L stainless steel. The results showed the MAF method effectively removed the majority of partially bonded particles and balling defects. In the same year, Arora and Singh [11] introduced a theoretical model to predict material removal volume and surface roughness reduction in the straight bevel (SB) new magnetorheological (MR) bevel gear finishing (BGF) method for gears. Surface roughness decreases from 450–90nm after 90 minutes of MR finishing, improving surface morphology as well as eliminating initial grinding marks and cracks. Ahmad et al. [12] explored the application of MAF for achieving defect-free micro/nano surface finishes, particularly focusing on challenging materials like the Ti-6Al-4V alloy. In 2023, Yan Wang et al. [13], using the fluid magnetic abrasives (FMA) polishing technique to improve the micro-shaft surface quality produced by the wire electrical discharge grinding (WEDG) process, removed recast layers, discharge craters, and micro-cracks. Results indicate significant surface roughness reduction and removal of recast layers, enhancing surface quality without micro-shaft deformation. In the same year, Li et al. [14] agreed with Yan Wang and showed the same result. In the same year, Rasouli and Nori [15] investigated the process parameter of MAF for refining the free surfaces of titanium blades. Results reveal that employing the magnetic abrasive method can reduce blade surface roughness by up to 33%.

Mechanism of MAF processes

MAF operates through the manipulation of MAPs under the influence of a magnetic field to refine the surface of a workpiece. Initially, a magnetic field is established between two poles, with the workpiece positioned within this field [16–20]. Within the gaps between the workpiece and the magnet, MAPs, comprising abrasive and magnetic particles, space is filled. As the magnetic field is activated, it aligns MAPs along its lines of force, shaping them into a pliable brush-like configuration [21–25]. This magnetic brush is then systematically traversed across the workpiece's surface, gently abrading and smoothing it by removing material [26–29].

Experiment setups

The study evaluated the use of B_4C as an abrasive powder in the MAF process, focusing on eliminating fatigue crack layers from metallic surfaces to improve component durability and reliability under cyclic loads. The Taguchi methodology was used to design a frame manuscript for simulating controlled finishing conditions and analyzing interactions between abrasive particles as well as fatigue crack layers in nine experiments, as indicated in Table 1. Table 2 showed the constant parameters of the process condition, while Figure 1 presented in the block diagram for the computational algorithm for the MAF.

Tool preparation (coil, pole)

The MAF process involves selecting raw materials, like ferromagnetic solid shafts and insulated copper wire. The shaft is cleaned using a Turing machine, and critical components like slip rings and plastic rolls are installed. A plastic insulating roll is employed to separate the electrical connection between the lip and the coil. The slip rings facilitate the transfer of electrical power

from the stationary wire to the rotating shaft, as illustrated in Figure 2.

Workpiece preparation

A compressor blade for a gas turbine from General Electric Company (GE) model frame 9E was chosen. The compressor blade is regarded as a critical and consumable component in gas turbines due to its intricate geometric design, elevated manufacturing costs, the specific alloy utilized, as well as its resistance to corrosion, thermal stresses, and cyclic loading. Moreover, the dominance of manufacturing companies in the reconditioning process necessitates an examination of the blade design and the formulation of appropriate strategies to prolong its lifespan. Figure 3 illustrates the compressor blades utilized in frame 9 from General Electric. Owing to the challenge

of acquiring a compressor blade, one blade was procured and segmented into nine samples measuring 30 × 10 mm. Table 3 below presents the chemical composition of the AISI 403 stainless steel [35], utilized in the manufacture of compressor blades and turbines.

Methods used to analyze tests

1. Specimen preparation
- Workpiece Material: AISI 403 stainless steel, commonly used in gas turbine compressor blades.
- Specimen geometry: Flat surfaces (30 × 10 × 5 mm) were cut from a single compressor blade to ensure uniformity.
- Pre-MAF condition: Specimens exhibited surface roughness (Ra) and micro-cracks due to prior machining and cyclic stresses.

2. Equipment and setup
- MAF tool:
- Coil: Pure copper wire (5200 turns, 0.6 mm diameter) powered by a 48V supply.
- Tool type: Stainless steel shaft with slip rings for electrical connectivity.
- Machining platform: Drilling machine (Taksan model) adapted for rotational MAF.
- Abrasive particles: B_4C with a grain size of 300 μm, mixed at ratios of 30%, 40%, and 50%.
- Magnetic field: Generated via the coil, aligning magnetic abrasive particles (MAPs) into a flexible "brush" for finishing.

3. Process parameters
- Variable parameters (Taguchi Design):
- Tool rotation speed: 400, 630, 800 rpm.
- Gap distance: 1.3, 1.8, 2.3 mm (between workpiece and tool).
- Abrasive mixing ratio: 30%, 40%, 50%.
- Constant parameters:
- Finishing time: 10 minutes.
- Voltage: 48 V.
- Abrasive grain size: 300 μm.

4. Measurement techniques:
- Surface roughness (SR): Measured using a profilometer before and after MAF Improvement using a portable device (VTSYIQI). Calculated according Equation 1
- Surface topology: Analyzed via light microscopy (Figure 4) to assess the maximum possible surface area from crack removal and uniformity at the Metallurgy Laboratory of the Production and Metallurgy Engineering
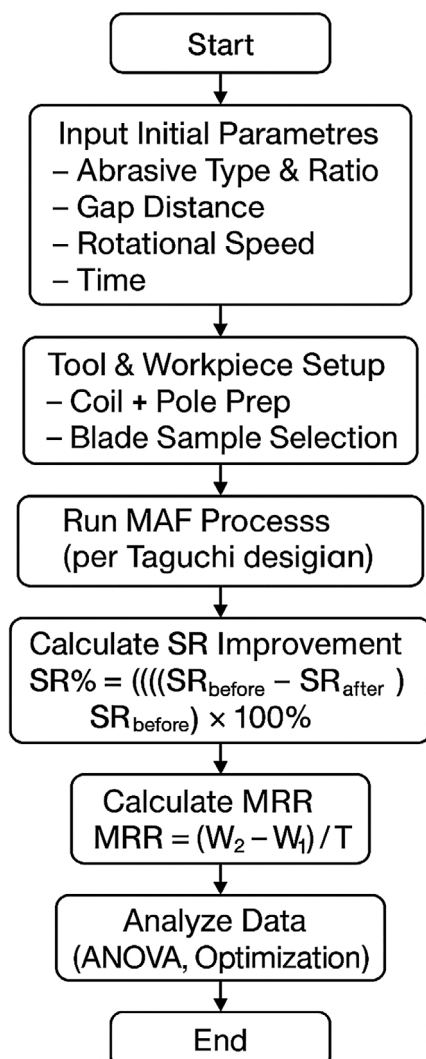

Figure 1. Block diagram: Computational algorithm for MAF process

Table 1. The parameters change of MAF process and Taguchi designs levels

Input parameter	Levels			Unit
	Level 1	Level 2	Level 3	
Tool rotation speed	400	630	800	rpm
Gab distance	1.3	1.8	2.3	mm
Abrasive mixing ratio	30	40	50	%

Table 2. The constant parameters process condition

Parameters	Discription
Voltage supply	48 V
Coil properties	Pure copper (5200) no. of turns, (0.6) mm is diameter of coil
Finishing time	10 min
Workpiece type	AISI 403 stainless steel
Tool type	Stainless steel
Workpiece dimension	(30×10×5) mm flat surface
Abrasive grain size	300 um
Machining	Drilling machine (taksan model) was used.
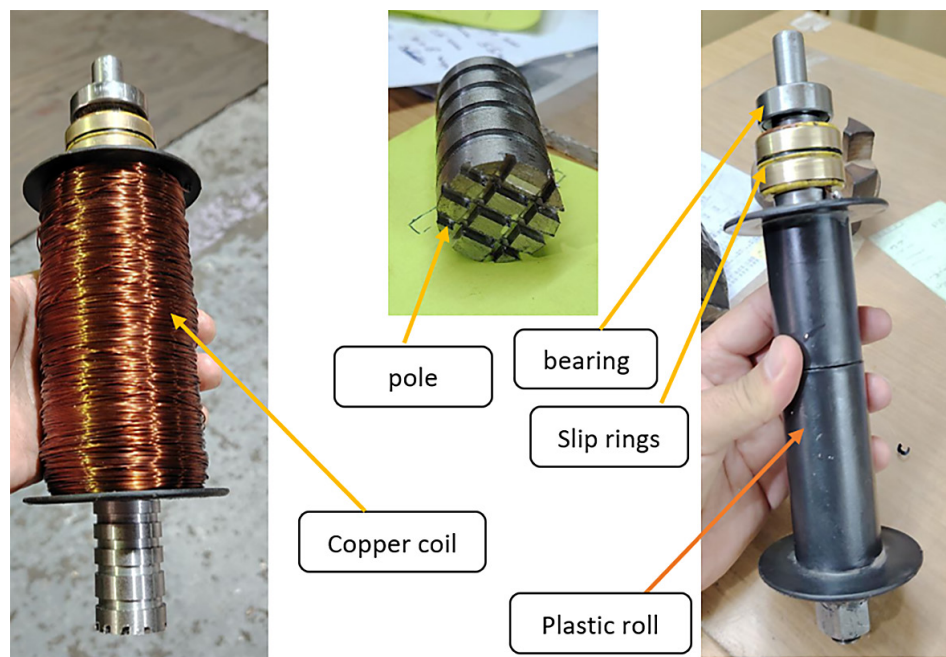
Figure 2. The stationary wire and the rotating shaft

Department at the University of Technology Baghdad, Iraq.

5. Statistical analysis
- Taguchi methodology: L9 orthogonal array for 3 factors at 3 levels (9 experiments). ANOVA to determine parameter significance (e.g., mixing ratio had the highest F-value for SR improvement).

RESULTS AND DISCUSSION

This research provides significant insights for component design engineers by illustrating the efficacy of MAF in improving the surface integrity of essential components, including gas turbine compressor blades. The research demonstrates that MAF substantially diminishes surface roughness and efficiently eliminates the fatigue-induced

Table 3. Chemical composition of AISI 403 stainless steel

Element	C	Si	Mn	Cr	Ni	P	S	Fe
AISI 403	0.15	0.50	1.0	11.5-13	…	0.04	0.03	Balance

Figure 3. Compressor blades of frame 9 from GE company
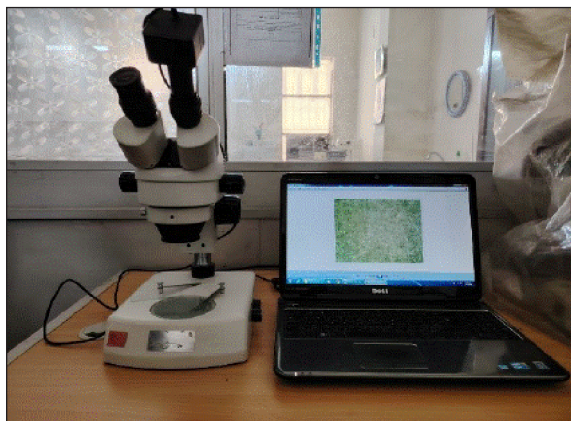
Figure 4. The lighting microscope used to show surface topology

microcracks, which are critical issues in high-stress applications. These enhancements directly enhance fatigue life, operational reliability, and overall component efficacy. The application of Taguchi methodology for optimizing process parameters offers a systematic framework that engineers can utilize in the design phase to guarantee components are both high-performing and manufacturable with exceptional surface quality. The results underscore the appropriateness of employing MAF for intricate geometries and inaccessible surfaces, providing an effective finishing solution for complex or additively manufactured components. The study proposes scalable finishing methods that allow for the concurrent processing of multiple components, which enhances cost-effective production and maintenance strategies. The findings endorse the incorporation of MAF into the design and refurbishment process, assisting engineers in producing more resilient, reworkable, and high-precision components.

Three measurements of surface roughness (SR) were obtained, and their average was calculated. The percentage enhancement of %SR was calculated using equation (1). The material removal rate (MRR) for each specimen was calculated using equation (2). Time is invariant; thus, it is exclude from the MRR equation 1

$$SR\% = \frac{SR\ after - SR\ before}{SR\ before} \times 100\% \qquad (1)$$

where: *SR%* – Surface improvement ratio, *SR after* – after MAF, process, *SR before* – before process MAF.

$$MRR = (W_2 - W1)/T \qquad (2)$$

where: *MRR* – Material removal rate, W_2 – weight before MAF process, W_1 = weight after MAF process, *T* – time of the process.

Figure 5 presents SEM fractography images analyzed to examine the surface morphology. The images offered significant insights into the failure mechanisms, highlighting aspects such as crack initiation sites, propagation pathways, and the impact of surface irregularities. The SEM analysis corroborated the findings by validating the nature and magnitude of surface damage under various machining conditions.

Surface roughness

Utilizing Taguchi design, 9 samples were obtained, as illustrated in Table 4. The principal effects plot for SR, depicted in Figure 6, demonstrates that speed has a non-linear impact, with the
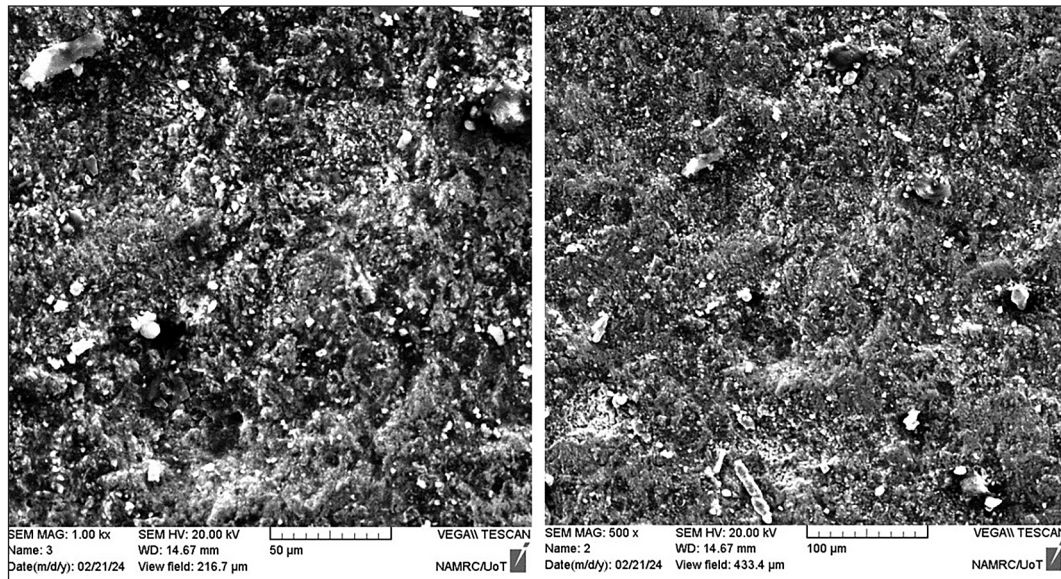
Figure 5. SEM fractography showing surface morphology and failure features, including crack initiation points and surface irregularities

average value increasing from 400 to 630 r.p.m., indicating improved performance, followed by a significant decrease at 800 r.p.m. This indicates that 630 r.p.m. is an optimal velocity, presumably owing to a balance between adequate rotational energy and process stability. The gap distance exhibits a distinct peak at 1.8 mm, with diminished performance at both 1.3 mm and 2.3 mm. This indicates that an intermediate gap facilitates optimal interaction between the magnetic field and abrasive particles, resulting in superior outcomes. Ultimately, the mixed abrasive ratio exhibits the highest mean at 30%, with a decrease noted at elevated percentages of 40% and 50%. This may result from the congestion of abrasive particles or a decline in magnetic control over them, adversely impacting the finishing quality. The most substantial SR improvement was 38.66, indicating a

remarkable advancement relative to an alternative abrasive particle. The analysis of variance for SR is presented in Table 5, indicating that the mixing ratio exerts the most significant influence.

Surface topology

MAF significantly improves surface topology. Before the MAF, surfaces usually have high roughness values (Ra), wear, and micro-level peaks and valleys from earlier forming or machining operations. Also, the surfaces have microcracks due to applied cycle stresses, which negatively affect functional performance. Subsequent to MAF, the abrasive interaction of magnetic particles and abrasives refines the surface, diminishing peaks and leveling valleys to attain a consistent and polished finish, resulting in

Table 4. Taguchi design for the 3 different parameters and output response

NO. Of specimen	Speed (r.p.m)	Gab distance (mm)	Mixed abrasive ratio (%)	SR before process	SR after process	SR μm improvement (%)	MRR (g)
1	400	1.3	50	0.82	0.709	13.455	0.0034
2	400	1.8	40	0.781	0.57	26.84	0.0038
3	400	2.3	30	0.802	0.630	21.36	0.0028
4	630	1.3	40	0.675	0.57	15.308	0.0083
5	630	1.8	30	0.864	0.698	19.174	0.0013
6	630	2.3	50	1.1	0.861	21.72	0.0057
7	800	1.3	30	0.91	0.824	9.450	0.0039
8	800	1.8	50	1.243	0.758	38.99	0.0034
9	800	2.3	40	0.843	0.62	26.453	0.0049

Table 5. Analysis of variance for SR

Source	DF	Adj SS	Adj MS	F-Value	P-Value
Regression	3	0.011329	0.003776	0.70	0.591
Rotation speed	1	0.004404	0.004404	0.82	0.408
Gap	1	0.000192	0.000192	0.04	0.858
Mixing ratio	1	0.006733	0.006733	1.25	0.315
Error	5	0.026988	0.005398		
Total	8	0.038318			
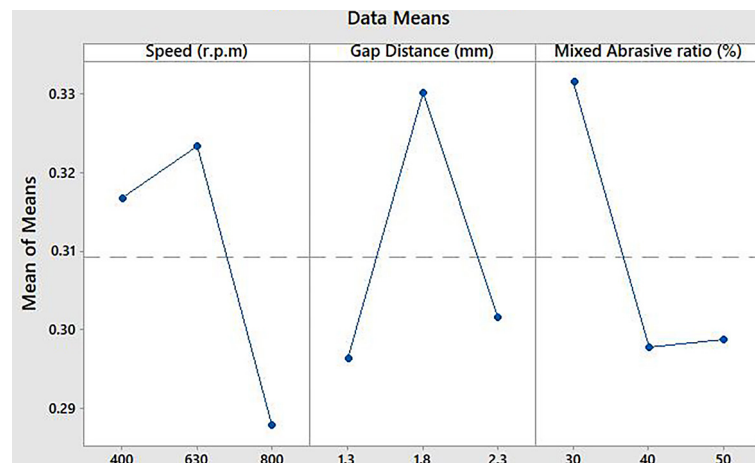
Figure 6. Main effects plot for surface roughness (SR)

markedly reduced roughness values. The best SR improvement was 38.99, while the lowest SR improvement was 9.45. Surface topology observations with a light microscope were undertaken at the Metallurgy Laboratory of the Production and Metallurgy Engineering Department at the University of Technology Baghdad-Iraq to elucidate the surface topography and minute fissures over the maximum feasible region. The MAF process is appropriate for intricate geometric configurations and expensive manufacturing, as it eliminates microcracks and attains stringent tolerances. Table 7 illustrates the variation in surface topology prior to and subsequent to the application of the MAF process on the samples. Table 6 highlights the surface enhancements, process parameters, and MAF type used in the MAF process in literature studies compared with this study. These include a decrease in surface roughness, ultra-smooth surfaces with Ra values below 0.1 µm, and enhanced surface uniformity. The procedure also eliminates micro-cracks and burrs, polishes edges, and eliminates subsurface flaws. It generates compressive residual stresses, improves fatigue life, and elevates surface hardness through abrasive work hardening. The smoother surfaces also enhance corrosion resistance. This study illustrates the effective elimination of micro-cracks from intricately curved turbine blades, enhancing surface roughness, prolonging component lifespan, and enabling timely rehabilitation prior to substantial damage. Table 7 illustrates colored circles that highlight micro-cracks and surface imperfections, including pits and protrusions, existing prior to the MAF process. The imperfections were effectively eliminated, and the surface was markedly enhanced following the application of MAF, as evidenced by the variations in surface topography pre- and post-processing. Nevertheless, in certain instances, no notable surface alterations were detected following MAF. This may be ascribed to fluctuations in the operational conditions during the MAF process or to the absence of significant cracks or surface degradation throughout their service life. Fluctuations in operational conditions during MAF can substantially influence the efficacy of surface enhancement.

Comparison of results

1. Optimal parameters:

Table 6. Compares between this work and other works by using MAF process

Aim of study	Description	MAF process type	Key Input parameters	Workpiece	Ref.
Using different abrasive fine-finishing technologies to reduced (Ra)	Best Ra was achieves ultra-smooth surfaces (Ra < 0.1 µm) at MAF.	Rotational MAF	- Magnetic flux: 0.5 T - Abrasive: SiC (5 µm) - RPM: 800 - Gap: 1.5 mm	T-15 steel, stainless steel (AISI 304)	[36]
Improved surface uniformity	Eliminates irregularities, creating a homogeneous surface.	Vibratory MAF	- Magnetic flux: 0.3 T - Abrasive: Diamond (3 µm) - Frequency: 50 Hz	Titanium alloy (Ti-6Al-4V)	[37]
Removal of micro-cracks and burrs	Polishes edges and removes subsurface defects.	Stationary MAF	- Magnetic flux: 0.7 T - Abrasive: Al_2O_3 (10 µm) - Feed rate: 5 mm/min	Tool steel (D2)	[38]
Compressive residual stresses	Enhances fatigue life by inducing beneficial residual stresses.	Hybrid MAF (ECM + MAF)	- Magnetic flux: 0.6 T - Abrasive: B_4C (7 µm) - Current: 2 A (ECM)	Nickel-based superalloy (Inconel 718)	[39]
Enhanced surface hardness	Work-hardens the surface layer due to abrasive action.	Linear MAF	- Magnetic flux: 0.4 T - Abrasive: SiO_2 (15 µm) - Speed: 0.2 m/s	Aluminum alloy (6061)	[40]
Improved corrosion resistance	Smoother surfaces reduce sites for corrosion initiation.	Ultrasonic-assisted MAF	- Magnetic flux: 0.2 T - Abrasive: CeO_2 (8 µm) - Ultrasonic power: 200 W	Magnesium alloy (AZ31B)	[41]
To extend the service life of gas turbine compressor blades	The process effectively removes microcracks and improves surface roughness, extending the part's service life and enabling rehabilitation before damage.	MAF for flat surface	- RPM = 400, 630,800 -Gap = 1.3 ,1.8 ,2.3 mm -Abrasive mixing ratio = 30% ,40% ,50%	Compressor blades turbine AISI 403 stainless steel	This study

- Best SR improvement (38.99%): Achieved at 800 rpm, 1.8 mm gap, and 50% abrasive ratio.

2. Surface quality vs. literature:
- This study achieved up to 38.99% SR improvement with B_4C, comparable to:
- Ultrasonic-assisted MAF (26% improvement on Ti-6Al-4V, Ref. [8]).
- Hybrid MAF-ECM (recast layer removal, Ref. [13]).
- Micro-Crack elimination: SEM confirmed removal of surface defects, aligning with findings in Ref. [9] and [15]

3. Process efficiency:
- Rotational MAF outperformed stationary methods (e.g., Ref. [36]) due to dynamic abrasive action).
- B_4C abrasives showed superior performance over SiC or Al_2O_3 in hardness-driven applications, Ref. [4].

4. Limitations:
- Non-linear effects at high speeds (800 rpm) reduced consistency.
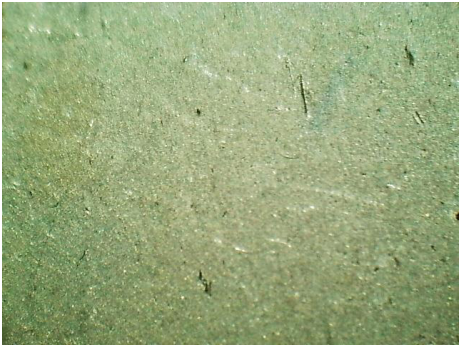- Smaller gaps (1.3 mm) increased MRR but risked abrasive congestion.
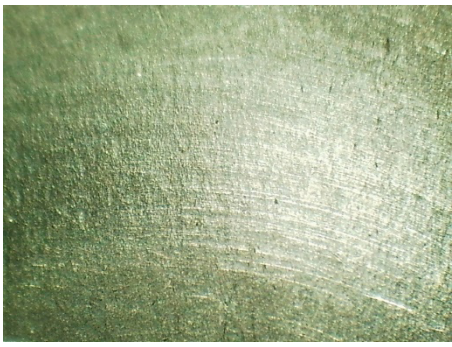
5. Essential insights
- Methodological robustness: The Taguchi design facilitated systematic optimization, corroborated by ANOVA.
- Practical implications: MAF combined with B_4C is effective for high-stress components (e.g., turbine blades), providing an 80% reduction in cracking and prolonging service life.
- Future work: Enhancing scalability for batch processing and integrating with additive manufacturing [7].
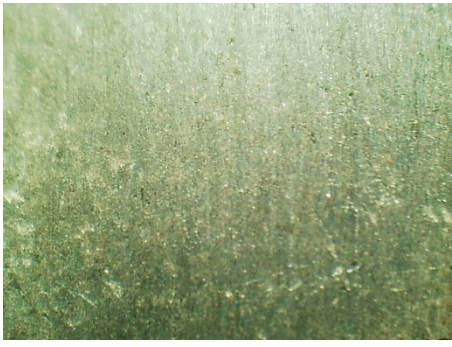
CONCLUSIONS

The study demonstrates the effectiveness of MAF with boron carbide abrasive powder in improving the surface quality of gas turbine compressor blades. It shows significant improvements in surface roughness and fatigue fracture elimination, with optimal results achieved at a rotational speed of 630 rpm and a 30% abrasive mixing ratio. The surface treatment process is deemed effective when applied prior to significant degradation and the deep propagation of surface cracks, which are often difficult to eliminate at advanced stages. Early intervention not only extends the service life of

Table 7. Comparison between surface topology before and after MAF

No.	Before MAF	After MAF
1		
2		
3		
4		
5		

the product and enhances its operational reliability but also contributes to a reduction in exclusive manufacturing costs. The following conclusions can be drawn from this research:

1. First, magnetic field abrasive finishing was used to enhance fatigue cracks (MAF for flat surfaces). Using surface microscopy, it was observed that the surface topography improved by approximately 80%. This improvement reflects a significant reduction in micro-cracks,

pits, and surface irregularities.

2. The best SR improvement was 38.99, achieved at a speed of 800 r.p.m., a gap distance of 1.8 mm, and a 50% mixed abrasive ratio. This indicates that increasing the velocity and the concentration of abrasive materials contributed to further improvement in the surface quality. A significant enhancement is evident in samples 1 to 7, as illustrated in Table 7.

3. Higher material removal occurs at a lower gap distance (1.3 mm) and a higher abrasive ratio (40%). Due to the hardness of the abrasive material, a smaller working gap resulted in a higher material removal rate, indicating that the abrasive particles interacted more effectively with the surface. ⌐

4. Suitable for geometries and high-precision applications in advanced manufacturing. ⌐

5. B₄C, due to its remarkable hardness and sharp cutting edges, enables improved surface quality (38.99–9.5%), which is favorable compared to other particles, thereby delivering superior surface finishing performance.

6. The researcher proposes running one or more turbine blades at the same time by creating a mathematical model that includes the shapes of blades, with the goal of maximizing efficiency quickly, while also being cost-effective and allowing for regular checks before and after use.

Acknowledgments

REFERENCES

1. Choopani Y., Razfar M. R., Saraeian P., and Farahnakian M., Experimental investigation of external surface finishing of AISI 440C stainless steel cylinders using the magnetic abrasive finishing process, International Journal of Advanced Manufacturing Technology, 2016, 83(9–12), 1811–1821, doi: 10.1007/s00170-015-7700-3.

2. Ahmed A., S. S.-E. R. Express, and undefined 2024, "Optimizing the five magnetic abrasive finishing factors on surface quality using Taguchi-based grey relational analysis," iopscience.iop.org, Accessed: Jan. 25, 2025. [Online]. Available: https://iopscience.iop.org/article/10.1088/2631-8695/ad2d99/meta

3. Rémy L., Geuffrard M., Alam A., Köster A., and Fleury E. Effects of microstructure in high temperature fatigue: Lifetime to crack initiation of a single crystal superalloy in high temperature low cycle fatigue, Int J Fatigue, 2013, 57, 37–49, doi: 10.1016/j.ijfatigue.2012.10.013.

4. Singh A. et al. Comparative assessment of abrasives in magnetic abrasive finishing: An experimental performance evaluation, J Magn Magn Mater, Aug. 2024, 604, 172312, doi: 10.1016/J.JMMM.2024.172312.

5. Jiang C. P., Masrurotin W., Wibisono A. T. et al. Enhancing internal cooling channel design in Inconel 718 turbine blades via laser powder bed fusion: A comprehensive review of surface topography enhancements, *Int. J. Precis. Eng. Manuf.*, 2025, 26, 487–511, doi: 10.1007/s12541-024-01177-3.

6. Zhou K., Chen Y., Du Z. W., and Niu F. L. Surface integrity of titanium part by ultrasonic magnetic abrasive finishing, International Journal of Advanced Manufacturing Technology, 2015, 80(5–8), 997–1005, doi: 10.1007/s00170-015-7028-z.

7. [Khangura S. S., Sran L. S., Srivastava A. K., and Singh H. Investigations into the removal of edm recast layer with magnetic abrasive machining, ASME 2015 International Manufacturing Science and Engineering Conference, MSEC 2015, 2015, 1, 1–6.

8. Guo J., Tan Z. E., Au K. H., and Liu K. Experimental investigation into the effect of abrasive and force conditions in magnetic field-assisted finishing, International Journal of Advanced Manufacturing Technology, 2017, 90(5–8), 1881–1888, doi: 10.1007/s00170-016-9491-6.

9. Zhang J., Chaudhari A., and Wang H. Surface quality and material removal in magnetic abrasive finishing of selective laser melted 316L stainless steel, J Manuf Process, February 2019, 45, 710–719, doi: 10.1016/j.jmapro.2019.07.044.

10. Wu P. Y., Hirtler M., Bambach M., and Yamaguchi H. Effects of build- and scan-directions on magnetic field-assisted finishing of 316L stainless steel disks produced with selective laser melting, CIRP J Manuf Sci Technol, 2020, 31(2019), 583–594, doi: 10.1016/j.cirpj.2020.08.010.

11. Zhang Z. et al. Fatigue life enhancement in alpha/beta Ti–6Al–4V after shot peening: An EBSD and TEM crystallographic orientation mapping study of surface layer, Materialia (Oxf), 2020, 12, 100813, doi: 10.1016/j.mtla.2020.100813.

12. Takesue S., Kikuchi S., Akebono H., Morita T., and Komotori J. Characterization of surface layer formed by gas blow induction heating nitriding at different temperatures and its effect on the fatigue properties of titanium alloy, Results in Materials, 2020, 5, 100071, doi: 10.1016/j.rinma.2020.100071.

13. Schneller W., et al. Fatigue strength assessment of additively manufactured metallic structures considering bulk and surface layer characteristics, Addit Manuf, 2021, 40, 101930, doi: 10.1016/j.addma.2021.101930.

14. Arora K. and Singh A. K. Theoretical and experimental investigation on surface roughness of straight bevel gears using a novel magnetorheological finishing process, Wear, 2021, 476, no. December 2020, doi: 10.1016/j.wear.2021.203693.

15. Ahmad S., Singari R. M., and Mishra R. S. Development of Al2O3-SiO2-based magnetic abrasive by sintering method and its performance on Ti-6Al-4V during magnetic abrasive finishing, Transactions of the Institute of Metal Finishing, 2021, 99(2), 94–101, doi: 10.1080/00202967.2021.1865644.

16. Wang Y., Tang C. C., Chai H. Y., Chen Y. Z., Jin R. Q., and Xiong W. Study on removal of recast layer of NiTi shape memory alloy machined with magnetic field-assisted WEDM-ECM complex process, International Journal of Advanced Manufacturing Technology, 2023, 129(9–10), 4335–4354, doi: 10.1007/s00170-023-12588-3.

17. Li Z., Jia J., Wang Y., Lv M., and Yang S. Experimental study on polishing of fluid magnetic abrasives for the wire electrical discharge grinding surface of micro-shafts, International Journal of Advanced Manufacturing Technology, 2023, 129(5–6), 2067–2085, doi: 10.1007/s00170-023-12425-7.

18. Gottwalt-Baruth A., Kubaschinski P., Waltz M., and Tetzlaff U. Influence of the cutting method on the fatigue life and crack initiation of non-oriented electrical steel sheets, Int J Fatigue, 2024, 180, September 2023, 108073, doi: 10.1016/j.ijfatigue.2023.108073.

19. Rasouli S. A. and Nori D. Investigation of Mass Magnetic Abrasive Finishing Process on Compressor Blades, 2024, 12(4), 5–26.

20. Gao Y., Zhao Y., Zhang G., Yin F., Zhao G., and Guo H. Characteristics of a novel atomized spherical magnetic abrasive powder, International Journal of Advanced Manufacturing Technology, 2020, 110(1–2), 283–290, doi: 10.1007/s00170-020-05810-z.

21. Zou Y., Xie H., and Zhang Y. Study on surface quality improvement of the plane magnetic abrasive finishing process, International Journal of Advanced Manufacturing Technology, 2020, 109(7–8), 1825–1839, doi: 10.1007/s00170-020-05759-z.

22. Du Z. W., Chen Y., Zhou K., and Li C. Research on the electrolytic-magnetic abrasive finishing of nickel-based superalloy GH4169, International Journal of Advanced Manufacturing Technology, 2015, 81(5–8), 897–903, doi: 10.1007/s00170-015-7270-4.

23. Zou Y., Satou R., Yamazaki O., and Xie H. Development of a new finishing process combining a fixed abrasive polishing with magnetic abrasive finishing process, Machines, 2021, 9(4), 1–14, doi: 10.3390/machines9040081.

24. Zou Y., Xing B., and Sun X. Study on the magnetic abrasive finishing combined with electrolytic process—investigation of machining mechanism, International Journal of Advanced Manufacturing Technology, May 2020, 108(5–6), 1675–1689, doi: 10.1007/S00170-020-05442-3.

25. Ahmed, A. S. S.-E. R. Express, and undefined 2024, Optimizing the five magnetic abrasive finishing factors on surface quality using Taguchi-based grey relational analysis, iopscience.iop.org, Accessed: Jan. 25, 2025. [Online]. Available: https://iopscience.iop.org/article/10.1088/2631-8695/ad2d99/meta

26. Guo J. et al. Novel rotating-vibrating magnetic abrasive polishing method for double-layered internal surface finishing, Elsevier J Guo, KH Au, CN Sun, MH Goh, CW Kum, K Liu, J Wei, H Suzuki, R Kang Journal of Materials Processing Technology, 2019•Elsevier, Accessed: Jan. 25, 2025. [Online]. Available: https://www.sciencedirect.com/science/article/pii/S0924013618304217

27. Jain V. K. Abrasive-based nano-finishing techniques: An overview, Machining Science and Technology, 2008, 12(3), 257–294, doi: 10.1080/10910340802278133.

28. Babu M. K. and Chetty O. V. K. A study on recycling of abrasives in abrasive water jet machining, 2003, 254, October 2002, 763–773, doi: 10.1016/S0043-1648(03)00256.

29. Hashimoto F., Yamaguchi H., Krajnik P., Wegener K., Chaudhari R., Hoffmeister H. W. Abrasive fine-finishing technology. CIRP Annals, 2016, 65(2), 597–620.

30. Jain V. K., et al. Advanced magnetic abrasive finishing for nanoscale surface integrity. Journal of Manufacturing Processes, 2018, 35, 685–699.

31. Singh, D. K., Shan, H. S. Development of magneto-abrasive finishing process. International Journal of Machine Tools and Manufacture, 2002, 42(8), 953–959.

32. Yamaguchi, H., Shinmura, T., Ikeda, R. Study of internal finishing of austenitic stainless steel capillary tubes by magnetic abrasive finishing. Journal of Manufacturing Science and Engineering, 2017, 139(3), 031018.

33. Kremen, G. Z., Elsayed, E. A., Rafalovich, V. Mechanism of material removal in magnetic abrasive finishing. Wear, 2014, 317(1–2), 153–161.

34. Kala, P., Pandey, P. M. Comparison of finishing characteristics of two paramagnetic materials using MAF. International Journal of Advanced Manufacturing Technology, 2015, 77(5–8), 997–1010.